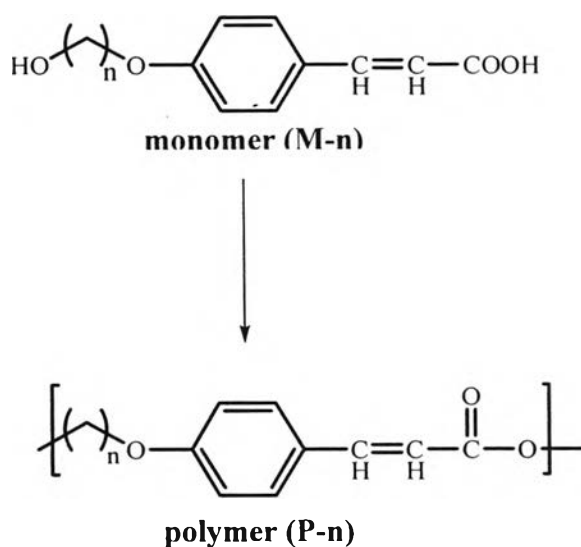


## CHAPTER III

### RESULTS AND DISCUSSION

In this thesis, oligomeric/polymeric material with chromophoric structural component that can absorb UV light was the synthesis goal. To do so, monomeric units with UV absorption property were created. Since cinnamate is a class of UV filtering agent used world-wide, monomers based on cinnamate structure were pursued in this work. Although a commercially available *p*-hydroxy cinnamic acid contains both hydroxyl and carboxyl group ready for esterification into a polymer, condensation of *p*-hydroxy cinnamic acid would yield polymer that can form a long conjugation system easily. Moreover, upon condensation of hydroxyl group on benzene ring will be changed which will affect strongly the photo-absorption property of the compound. Therefore, we have synthesized *p*-alkoxycinnamic acid with various carbon chain lengths at the alkoxy moiety together with a hydroxyl group at the termini of the alkoxy moiety. This bifunctional monomer could then be condensed into polyester containing UV absorptive chromophores the structural units.



### 3.1 Syntheses of monomers

The syntheses of four monomers were done through alkylation between one mole equivalent of *p*-hydroxycinnamic acid and various mole equivalents of bromo alkyl alcohol as depicted in Table 3.1 using potassium carbonate as catalyst.

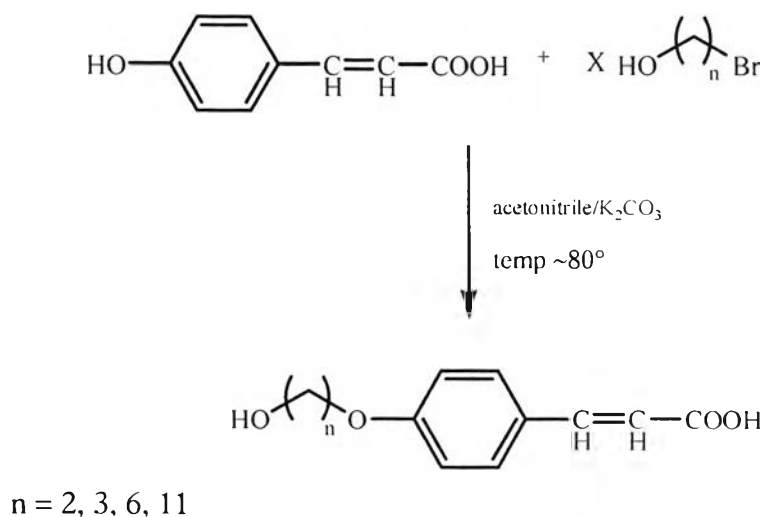


**Table 3.1** Reaction conditions for synthesis of monomers

monomer	n	Mole equivalent of bromo-alkyl alcohol	Reaction Time (hours)
<i>p</i> -(2-hydroxy ethoxy) cinnamic acid	2	10	36
<i>p</i> -(3-hydroxy propoxy) cinnamic acid	3	5	27
<i>p</i> -(6-hydroxy hexyloxy) cinnamic acid	6	3	40
<i>p</i> -(11-hydroxy undecyloxy) cinnamic acid	11	3	40

The structures of all four monomers were characterized using various spectroscopic techniques including  $^1\text{H}$ ,  $^{13}\text{C}$ -NMR and IR spectroscopy (see Appendix B). Table 3.2 shows solubility property of the synthesized monomers. It can be seen that different monomers possess different solubility properties resulting from the different of their chemical structures.

**Table 3.2** Solubility property of the synthesized monomers

solvent	M-2	M-3	M-6	M-11
water	+-	+-	--	--
acetonitrile	++ <sup>a</sup>	+-	+-	+-
methanol	++	++	++	++
acetone	++	++	++	++
ethyl acetate	+ <sup>a</sup>	++ <sup>a</sup>	++	++
chloroform	+-	+-	+-	+-
dichloromethane	--	--	--	--
diethyl ether	--	--	--	--
toluene	-- <sup>a</sup>	++ <sup>a</sup>	++ <sup>a</sup>	++ <sup>a</sup>
hexane	--	--	--	--

<sup>a</sup> means after heated

-- insoluble, +- partially soluble, ++ soluble

Experiment were done to obtain UV absorption properties ( $\lambda_{\max}$  and  $\epsilon$ ) of all the monomers. As shown in Figure 3.1, all four monomers showed similar UVB absorption band. This agreed well with the fact that all four monomers contained similar chromophoric moiety. The difference among these four monomers lied at the non-chromogenic-carbon chain connecting two cinnamate together. As mentioned earlier, these carbon chain length although affected the solubility property but had no influence in UV absorption property of the molecule.

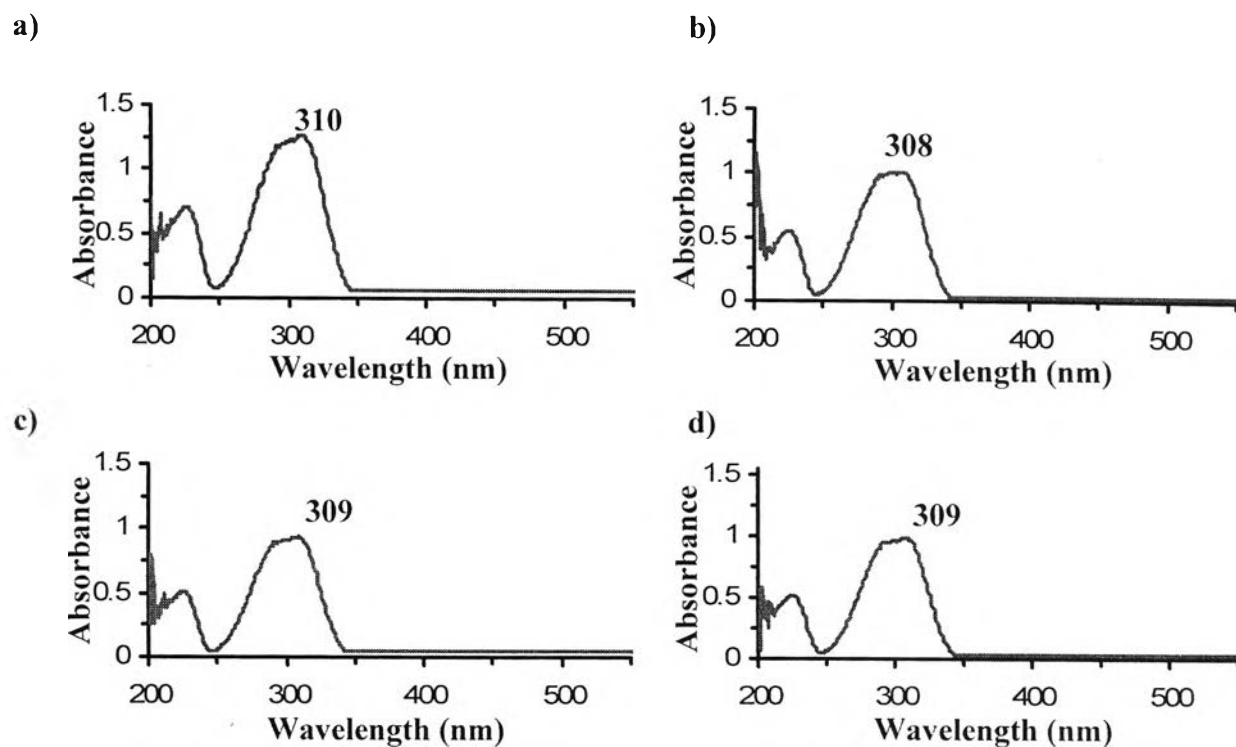


**Figure 3.1** UV spectra of a) M-2, b) M-3, c) M-6 and d) M-11

By plotting a graph between absorbances (at  $\lambda_{\max}$ ) and concentrations of each monomer sample, a linear relationship was obtained with its slope represented molar absorption coefficient value ( $\epsilon$ ) of the monomer. Table 3.3 shows  $\lambda_{\max}$  and  $\epsilon$  of each monomer. It can be seen that all four monomers gave comparable  $\epsilon$  and  $\lambda_{\max}$ .

**Table 3.3** UV spectral data of monomers in methanol

compound	$\lambda_{\max}$	$\epsilon$ ( $M^{-1}cm^{-1}$ )
M-2	310	26,000
M-3	308	27,000
M-6	309	25,000
M-11	309	26,000

### 3.2 Syntheses of polymers

Two types of polymers were prepared in this work; homopolymers and copolymers from 2 types of monomers. In addition, since *p*-toluene sulfonic acid could not successfully catalyze all the polymerization reactions in this work, other catalysts were also used during esterification of some monomers.

#### 3.2.1 Homopolymer

##### 3.2.1.1 Polymerization with *p*-toluene sulfonic acid

Three monomers, *p*-(3-hydroxy propoxy) cinnamic acid (**M-3**), *p*-(6-hydroxy hexyloxy) cinnamic acid (**M-6**) and *p*-(11-hydroxy undecyloxy) cinnamic acid (**M-11**) were polymerized by esterification reaction using *p*-toluene sulfonic acid as a catalyst. All three polymers (**P-3**, **P-6** and **P-11**) were subjected to <sup>1</sup>H-NMR and IR spectroscopic analyses. <sup>1</sup>H-NMR spectrum of **P-3** (Figure B.23 P.70) shows –OCH<sub>2</sub>– resonances at 4.38, 4.22-4.09 and 3.87 while the –OCH<sub>2</sub>– protons in monomer resonance at 4.16 (–CH<sub>2</sub>–O–Ar) and 3.88 (HO–CH<sub>2</sub>–). These obvious changes in <sup>1</sup>H-NMR together with molecular weight information from gel filtration confirm that esterification has been taking places.

The shift of carbonyl signal from 1676 cm<sup>-1</sup> in **M-3** IR spectrum to 1708 cm<sup>-1</sup> in **P-3** spectrum indicated the presence of ester functional group. The C=O stretching vibration of the **P-3** ester is lower than regular carbonyl ester because of conjugation. The disappearance of broad absorption at 3000-3300 cm<sup>-1</sup> indicated no –COOH functionality.

Similar results were observed for **P-6** and **P-11**: <sup>1</sup>H-NMR spectrum of **P-6** (Figure B.27 P.74) shows –OCH<sub>2</sub>– resonances at 4.21, 3.92 and 3.60 while the –OCH<sub>2</sub>– protons in monomer resonance at 4.00 (–CH<sub>2</sub>–O–Ar) and 3.66 (HO–CH<sub>2</sub>–). <sup>1</sup>H-NMR spectrum of **P-11** (Figure B.30 P.77) shows –OCH<sub>2</sub>– resonances at 4.18, 3.95 and 3.64 while the –OCH<sub>2</sub>– protons in monomer resonance at 3.99 (–CH<sub>2</sub>–O–Ar) and 3.64 (HO–CH<sub>2</sub>–). The shift of carbonyl signal from 1668 cm<sup>-1</sup> in **M-6** and 1683 cm<sup>-1</sup> in **M-11** IR spectrum to 1709 cm<sup>-1</sup> in **P-6** and **P-11** spectrum indicated the presence ester functional group in the polymer chain.

Progress of the polymerization reaction was followed by analyzing molecular weight of the reaction mixture at various reaction times using gel filtration analyses. The growth of the polymer is depicted in Figure 3.2. Since there was some solid

precipitate out during the esterification process, both precipitated solid and solubilized product were analyzed.

**P-3**, poly(*p*-propoxy cinnamate), could be obtained by refluxing **M-3**, *p*-(3-hydroxy propoxy) cinnamic acid, in toluene using *p*-toluene sulfonic acid as a catalyst. With more reaction time, condensation polymerization gave **P-3** with increasing number average molecular weight ( $\overline{M}_n$ ). Maximum  $\overline{M}_n$  (2200) of soluble P-3 was obtained at about 200 hours. If the reaction was allowed to continue, more P-3 precipitated out from the reaction mixture. The soluble product left in the reaction mixture gave  $\overline{M}_n$  of 1500.

The gel filtration results indicated that chain growth occurred for all three polymers. As shown in Figure 3.1a, at 96 hours, polymerization reaction of M-3 gave soluble product with a number average molecular weight ( $\overline{M}_n$ ) of 1363. The maximum  $\overline{M}_n$  (~2200) obtained was at 200-240 hours of refluxing and after 240 hours, a lot more solid had precipitated out. Analyzing soluble polymer product obtained after 240 hours revealed  $\overline{M}_n$  of ~1500. The decrease of  $\overline{M}_n$  of the soluble product obtained after 240 hours comparing to the soluble product obtained at 200-240 hours probably indicated that products with  $\overline{M}_n$  of about 2200 had grown into insoluble material and had precipitated out. Such precipitation then diluted the soluble product in the reaction mixture, therefore, favored cyclization of the polymer molecules. The soluble polymer, therefore, stopped increasing their sizes. Unfortunately, insoluble products (precipitate) was not soluble in any organic solvents, therefore, NMR or gel filtration analysis could not be performed. The similarity between IR spectra of the insoluble products (Figure B.25 P.72) and IR spectra of the soluble products (Figure B.24 P.71) confirmed that the precipitate was actually poly(*p*-propoxy cinnamate). It can, therefore, be concluded that poly(*p*-propoxy cinnamate) with  $\overline{M}_n$  of about 1500 can be synthesized by esterification of *p*-(3-hydroxy propoxy) cinnamic acid.

Similar situations were found during the polymerization of *p*-(6-hydroxy hexyloxy) cinnamic acid, **M-6**, into poly(*p*-hexyloxy cinnamate), **P-6**, and *p*-(11-hydroxy undecyloxy) cinnamic acid, **M-11**, into poly(*p*-undecyloxy cinnamate), **P-11**. Results of **P-6** chain growth and **P-11** chain growth were shown in Figure 3.1b and c, respectively.

As shown in Figure 3.1b, at 42 hours, polymerization reaction of **M-6** gave soluble product with a number average molecular weight ( $\overline{M}_n$ ) of 3819. The maximum  $\overline{M}_n$  (~4600) obtained was at 120 hours of refluxing and after 120 hours, a lot more solid had precipitated out. Analyzing soluble polymer product obtained after 240 hours revealed  $\overline{M}_n$  of ~3500. The decrease of  $\overline{M}_n$  of the soluble product obtained after 240 hours comparing to the soluble product obtained at 120 hours probably indicated that products with  $\overline{M}_n$  of about 3500 had grown into insoluble material and had precipitated out. The similarity between IR spectra of the insoluble products and IR spectra of the soluble products confirmed that the precipitate was actually poly(*p*-hexyloxy cinnamate). It can, therefore, be concluded that poly(*p*-hexyloxy cinnamate) with  $\overline{M}_n$  of about 3500 can be synthesized by esterification of *p*-(6-hydroxy hexyloxy) cinnamic acid.

As shown in Figure 3.1c, at 22 hours, polymerization reaction of **M-11** gave soluble product with a number average molecular weight ( $\overline{M}_n$ ) of 2035. The maximum  $\overline{M}_n$  (~5400) obtained was at 192 hours of refluxing and trace solid had precipitated out. **P-11** has long chain carbon more than **P-3** and **P-6**, so **P-11** has good solubility in toluene. It can, therefore, be concluded that poly(*p*-undecyloxy cinnamate) with  $\overline{M}_n$  of about 5400 can be synthesized by esterification of *p*-(11-hydroxy undecyloxy) cinnamic acid.

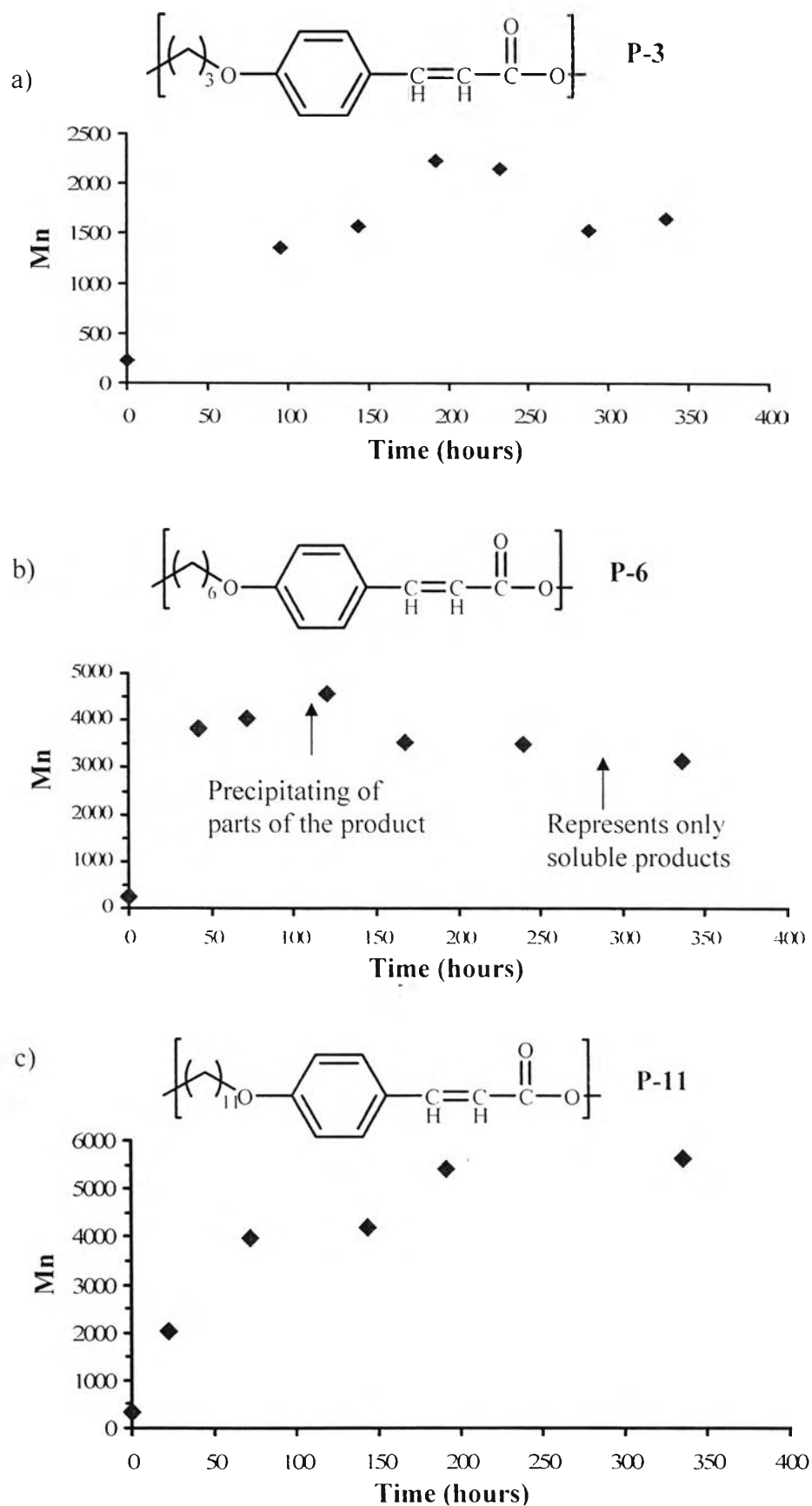


**Figure 3.2** Number average molecular weight and time relationship: (a) Poly(*p*-propoxy cinnamate), **P-3**; (b) Poly(*p*-hexyloxy cinnamate), **P-6** and (c) Poly(*p*-undecyloxy cinnamate), **P-11**



### Dilution system

As mentioned earlier that some insoluble products were formed during the polymerization reaction. To avoid such product, we must try to suppress the growth of polymer chains. To do so, dilution system was performed. In this system, polymerization was done at a lower monomer concentration. Cyclization should be a main route after most monomers were used up from the reaction mixtures.

*p*-(11-Hydroxy undecyloxy) cinnamic acid (M-11) was polymerized in toluene with *p*-toluene sulfonic acid using similar condition as described for the normal system. However, after 24h, toluene was added into the reaction in order to minimize chain growth and to maximize cyclization. Gel filtration analyzes revealed that at 72h of polymerization reaction, number average molecular weight of product was only 2511 comparing to 3971 for the nondilute reaction. Maximum cyclization at an early stage during polymerization also resulted in almost no precipitate during refluxing.

Polymer was also subjected to <sup>1</sup>H-MNR and IR spectroscopic analyses. <sup>1</sup>H-NMR spectrum shows -OCH<sub>2</sub>- resonances at 4.12, 3.86 and 3.56 while the protons in monomer resonance at 3.99 (-CH<sub>2</sub>-O-Ar) and 3.64 (HO-CH<sub>2</sub>-). The shift of carbonyl signal from 1683 cm<sup>-1</sup> in M-11 IR spectrum to 1708 cm<sup>-1</sup> in P-11 spectrum indicated that the ester functional group had been taking place. Both IR and NMR data also indicate that the P-11 contained neither carboxylic group nor hydroxyl functionality.

Experiments were done to obtain UV absorption properties ( $\lambda_{\max}$  and  $\epsilon$ ) of all the polymers. As shown in Figure 3.3, all three homopolymers (P-3, P-6 and P-11) show similar UVB absorption band. This agrees well with the fact that all three homopolymers contain similar chromophoric moiety.

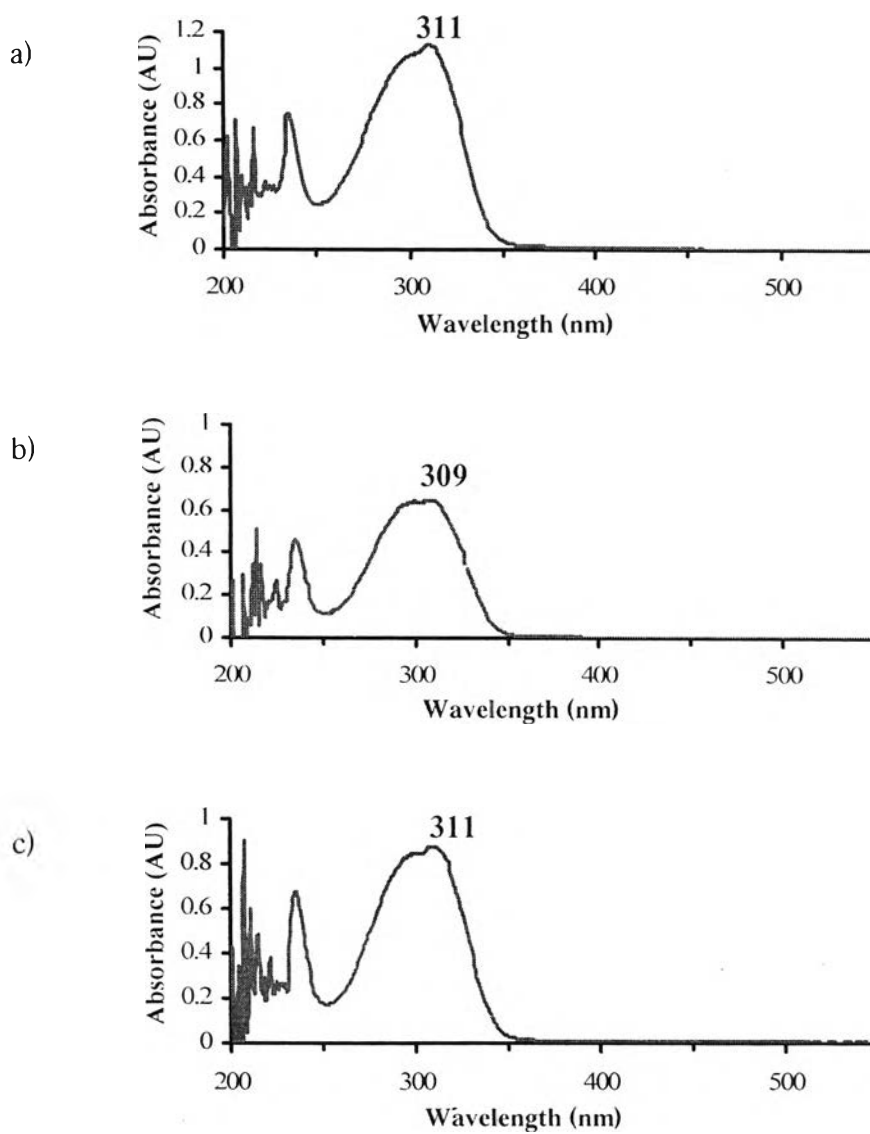


Figure 3.3 UV spectra of a) P-3, b) P-6 and c) P-11 in dichloromethane

Table 3.4 UV spectral data of homopolymers in dichloromethane

Compounds	$\lambda_{\max}$	$\epsilon$ ( $M^{-1}cm^{-1}$ )
P-3	311	26,000
P-6	309	23,000
P-11	311	20,000

### 3.2.1.2 Polymerization with coupling agent

The polymerization of *p*-(2-hydroxy-ethoxy)-cinnamic acid (**M-2**) could not be prepared in toluene with *p*-toluene sulfonic acid as a catalyst because this monomer was not soluble in toluene. Many experiments were tried including performing the reaction in both acetone and dry dimethylformamide in a presence of *p*-toluene sulfonic acid, Amberlyst-15 (cationic ion-exchange resin) and carrying a reaction in a presence of 1-(3-dimethylaminopropyl)-3-ethylcarbodiimide hydrochloride (EDCI) and 1-hydroxy-benzotriazole (HOBT) in dimethylformamide. The only successful method among those mentioned experiments was the use of *N,N'*-dicyclohexylcarbodiimide (DCC) as coupling agent. Because of poly(*p*-(2-ethoxy)cinnamate), **P-2**, was polymerized through this coupling method, contamination of *N,N'*-dicyclohexylurea (DCU) could not be avoided. As a result, the solubility test of **P-2** could not be observed. The number average molecular weight ( $\overline{M}_n$ ) of the product was 966.

$^1\text{H-NMR}$  Spectrum of **P-2** shows  $-\text{OCH}_2-$  resonances at 4.33, 4.13 and 3.98 ppm while the  $-\text{OCH}_2-$  protons in monomer resonance at 4.13 and 3.99 ppm.

Experiment was done to obtain UV absorption properties ( $\lambda_{\text{max}}$  and  $\epsilon$ ) of **P-2**. As shown in Figure 3.4, **P-2** shows UVB absorption band;  $\lambda_{\text{max}}$  of 312 nm. Molar absorptivity of this **P-2** could not be observed because of the contamination of DCU.

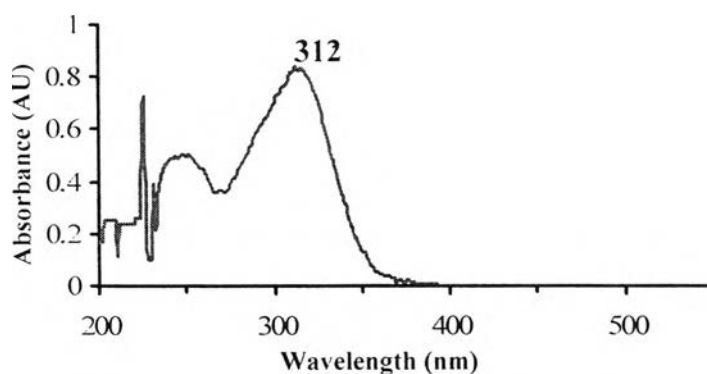


Figure 3.4 UV spectrum of **P-2** in dichloromethane

### 3.2.2 Copolymer

In order to obtain UV absorption polymer with different physico-chemical properties from **P-2**, **P-3**, **P-6** and **P-11**, copolymerization between **M-3** and **M-11** was done. The reason that **M-2** and **M-6** were not used is that **M-2** was difficult to polymerize and there was only a small amount of synthesized **M-6**.

### 3.2.2.1 Poly(*p*-propoxy cinnamate)-*co*-(*p*-undecyloxy cinnamate) (P-3/11)

An equal number of two monomers (M-3 and M-11) were polymerized in toluene using *p*-toluene sulfonic acid as catalyst. **M-11** was polymerized more rapidly than **M-3** so in this process **M-11** was added 2 times in 24 hours. The number average molecular weight of the copolymer was 2091. The solubility was shown in Table 3.4.

<sup>1</sup>H-NMR spectrum shows  $-\text{OCH}_2-$  resonances at 4.40-3.44 while the  $-\text{OCH}_2-$  protons in **M-3** resonance at 4.16 ( $-\text{CH}_2\text{-O-Ar}$ ), 3.88 ( $\text{HO-CH}_2-$ ) and **M-11** resonance at 3.99 ( $-\text{CH}_2\text{-O-Ar}$ ), 3.64 ( $\text{HO-CH}_2-$ ) indicated that the ester functional group had been taking place.

Experiment was done to obtain UV absorption properties ( $\lambda_{\text{max}}$  and  $\epsilon$ ) of P-3/11. As shown in Figure 3.5, **P-3/11** shows UVB absorption property;  $\lambda_{\text{max}}$  of 310 nm ( $\epsilon=20,000 \text{ M}^{-1} \text{ cm}^{-1}$ ).

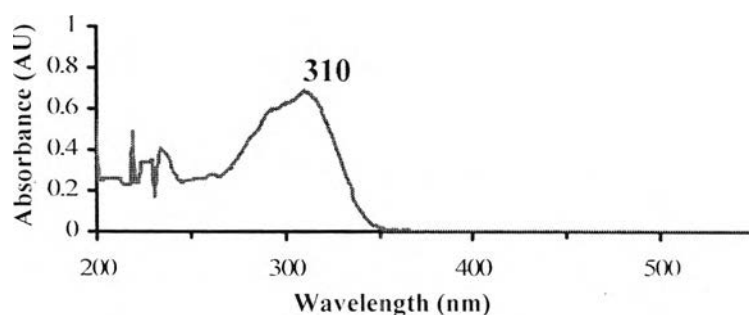


**Figure 3.5** UV spectrum of **P-3/11** in dichloromethane

### 3.2.2.2 poly(penta ethylene glycol cinnamate) (PPGC)

Since **P-2**, **P-3**, **P-6**, **P-11** and **P-3/11** are all solid material even at low Mn, changing polyethylene between the two cinnamate into polyethylene oxide might give product with different physical state.

As a result, copolymerization was done between one mole equivalent of *p*-hydroxycinnamic acid and two mole equivalents of pentaethylene glycol ditosylate in acetonitrile using potassium carbonate as a catalyst and tetrabutylammonium sulfate as a phase transfer. Polymer was also subjected to <sup>1</sup>H-NMR, <sup>13</sup>C-NMR and IR spectroscopic analyses. <sup>1</sup>H-NMR spectrum shows signal at 4.12 and 4.32 for  $-\text{CH}_2\text{-CH}_2\text{-O-Ar}$  and  $\text{Ar-CH=CH-COO-CH}_2-$  respectively. <sup>13</sup>C-NMR spectrum shows signal of  $\text{Ar-CH=CH-COO-CH}_2-$  at 167.2 ppm. The signals of aromatic carbons were detected at 114, 128, 130 and 161. For IR spectra, the absorption band around 2955-2856  $\text{cm}^{-1}$  corresponds to C-H stretching of aliphatic hydrocarbons and C=O

stretching vibration of ester functional group is at  $1707\text{ cm}^{-1}$ . The  $-\text{C}-\text{O}-\text{C}-$  stretching vibrations are shown at  $1172\text{ cm}^{-1}$ . Gel filtration analyses of reaction mixture at various reaction times gave a growth profile of PPGC polymerization (Figure 3.6).

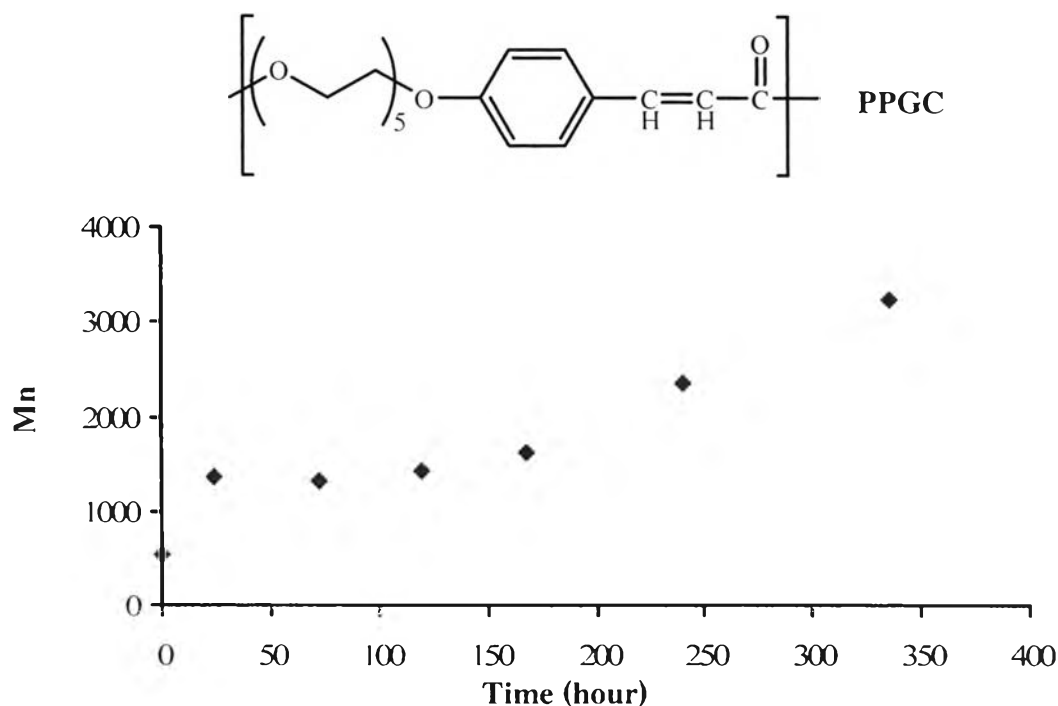


**Figure 3.6** Number average molecular weight and time relationship of poly(penta ethylene glycol cinnamate), PPGC

From the graph, it can be seen clearly that polymerization could take place steadily and chain growth kept continuing even at 2 weeks reaction time. This steady growth was a result of excellent solubility of the growing polymer chains. The outstanding characteristic of PPGC is that it is a light yellow oily liquid miscible with silicone fluids used in cosmetic industry (see Table 3.5 for solubility of **P-2**, **P-3**, **P-6**, **P-11**, **P-3/11** and **PPGC**).

Experiment was done to obtain UV absorption properties ( $\lambda_{\text{max}}$  and  $\epsilon$ ) of PPGC polymer. As shown in Figure 3.7, PPGC has one absorption band;  $\lambda_{\text{max}}$  of 310 nm ( $\epsilon = 27,000\text{ M}^{-1}\text{cm}^{-1}$ ) which correspond to the UVB region.

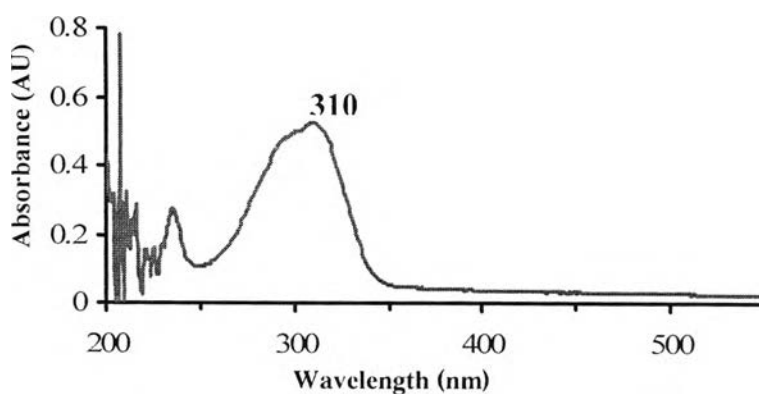


Figure 3.7 UV spectrum of PPGC in dichloromethane

Table 3.5 Solubility of the synthesized polymer

Solvent	P-3 ( $\bar{M}_n=1650$ )	P-6 ( $\bar{M}_n=3150$ )	P-11 ( $\bar{M}_n=5617$ )	PCO ( $\bar{M}_n=2091$ )	PPGC ( $\bar{M}_n=3250$ )
water	--	--	--	--	--
acetonitrile	+ <sup>a</sup>	+ <sup>a</sup>	+ <sup>a</sup>	+ <sup>-</sup>	++
ethanol	+ <sup>a</sup>	+ <sup>a</sup>	+ <sup>a</sup>	+ <sup>a</sup>	+ <sup>a</sup>
methanol	+ <sup>a</sup>	+ <sup>a</sup>	+ <sup>a</sup>	+ <sup>a</sup>	+ <sup>a</sup>
acetone	++ <sup>a</sup>	++ <sup>a</sup>	++ <sup>a</sup>	++	+ <sup>-</sup>
ethyl acetate	++	++ <sup>a</sup>	++ <sup>a</sup>	++	+ <sup>-</sup>
tetrahydrofuran	++	++	++	++	++
chloroform	++	++	++	++	++
dichlorometane	++	++	++	++	++
diethyl ether	+ <sup>-</sup>	++	++	++	--
toluene	++	++	++	++	--
hexane	--	--	--	--	--
DC200 <sup>b</sup>	-- <sup>a</sup>	-- <sup>a</sup>	-- <sup>a</sup>	-- <sup>a</sup>	++
DC556 <sup>c</sup>	ND	ND	ND	ND	++

-- insoluble, +- partially soluble, ++ soluble

ND not determine

<sup>a</sup> means after heated

<sup>b</sup> means linear polydimethylsiloxane polymers

<sup>c</sup> means phenyl trimethicone

### 3.3 Photostability Test

Four synthesized UV-filter polymers, **P-3**, **P-6**, **P-11**, **P-3/11** and **PPGC**, were subjected to photostability test. The tests were done in dichloromethane for 60 minutes at  $5.8 \text{ mW/cm}^2$  UVA and  $0.47 \text{ mW/cm}^2$  UVB irradiation. As shown in Figure 3.8, all five polymers showed comparable photostability with standard octyl methoxy cinnamate, a widely used UVB filter. The decrease of UV-absorbance of all five polymers was a result of *trans* to *cis* photoisomerization of the cinnamate moiety in the polymer. This was deduced from  $^1\text{H-NMR}$  of the irradiated samples.

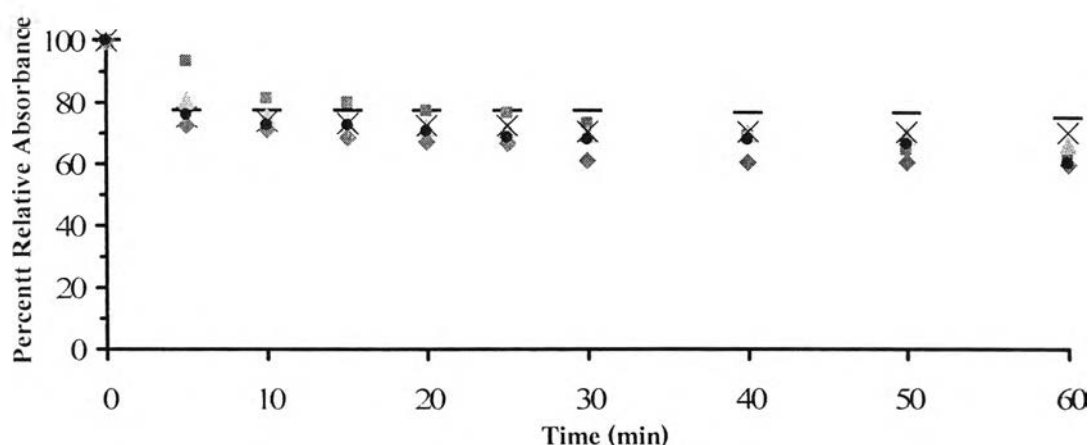


**Figure 3.8** Photostability of — octyl-p-methoxycinnamate (OMC), ■ P-3, ▲ P-6, × P-11, ♦ PPGC and • P-3/11 in dichloromethane

From Figure 3.8 it is obvious that PPGC is the least photo-stable. This is probably a result of hydrophilic nature of polyethylene oxide chain. Previous study has indicated that more *trans* to *cis* photoisomerization could be observed in more polar solvents.<sup>40</sup>

The decrease in UV absorption upon UV exposure agreed with the previous study<sup>40</sup> in OMC in which *trans* to *cis* isomerization was identified as a cause of such decrease. The  $^1\text{H-NMR}$  spectra of the polymer before and after UV-exposure were shown in Figure 3.9. Obvious *trans* to *cis* isomerization could be seen from these spectral pairs.

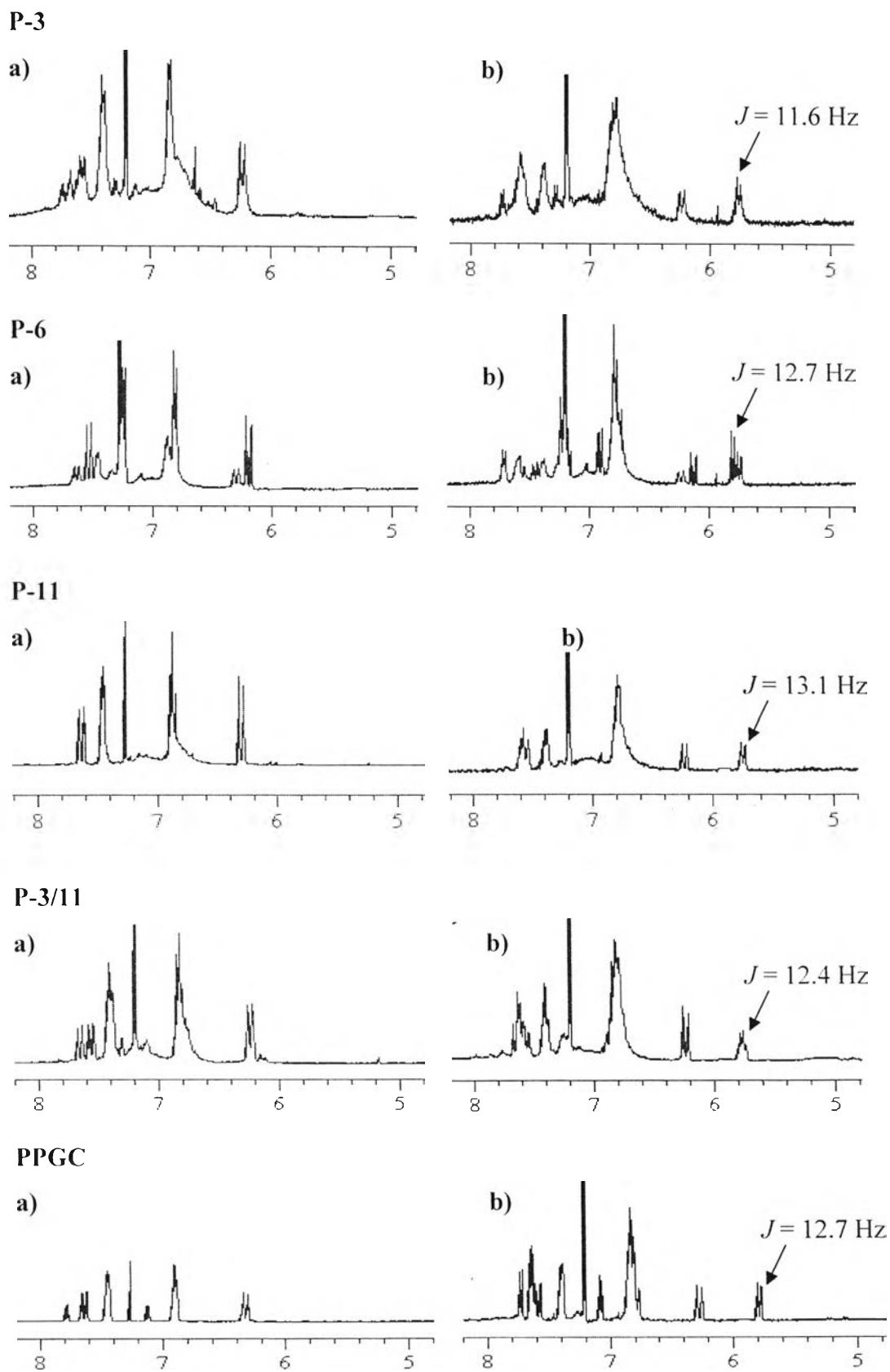


**Figure 3.9** <sup>1</sup>H-NMR spectra of **P-3**, **P-6**, **P-11**, **P-3/11** and **PPGC**: a) before UVA/UVB irradiation. b) after UVA/UVB irradiation; the irradiation was done for 60 min at 5.8 mW/cm<sup>2</sup> UVA and 0.47 mW/cm<sup>2</sup> UVB



### 3.4 Percutaneous Absorption Test

In *vitro* skin penetration of OMC and synthesized UV-filtering polymers are shown in Figure 3.10. The results indicated that all polymeric UV-filters could not penetrate a baby mice skin while a significant amount of OMC could penetrate such skin easily and quickly.

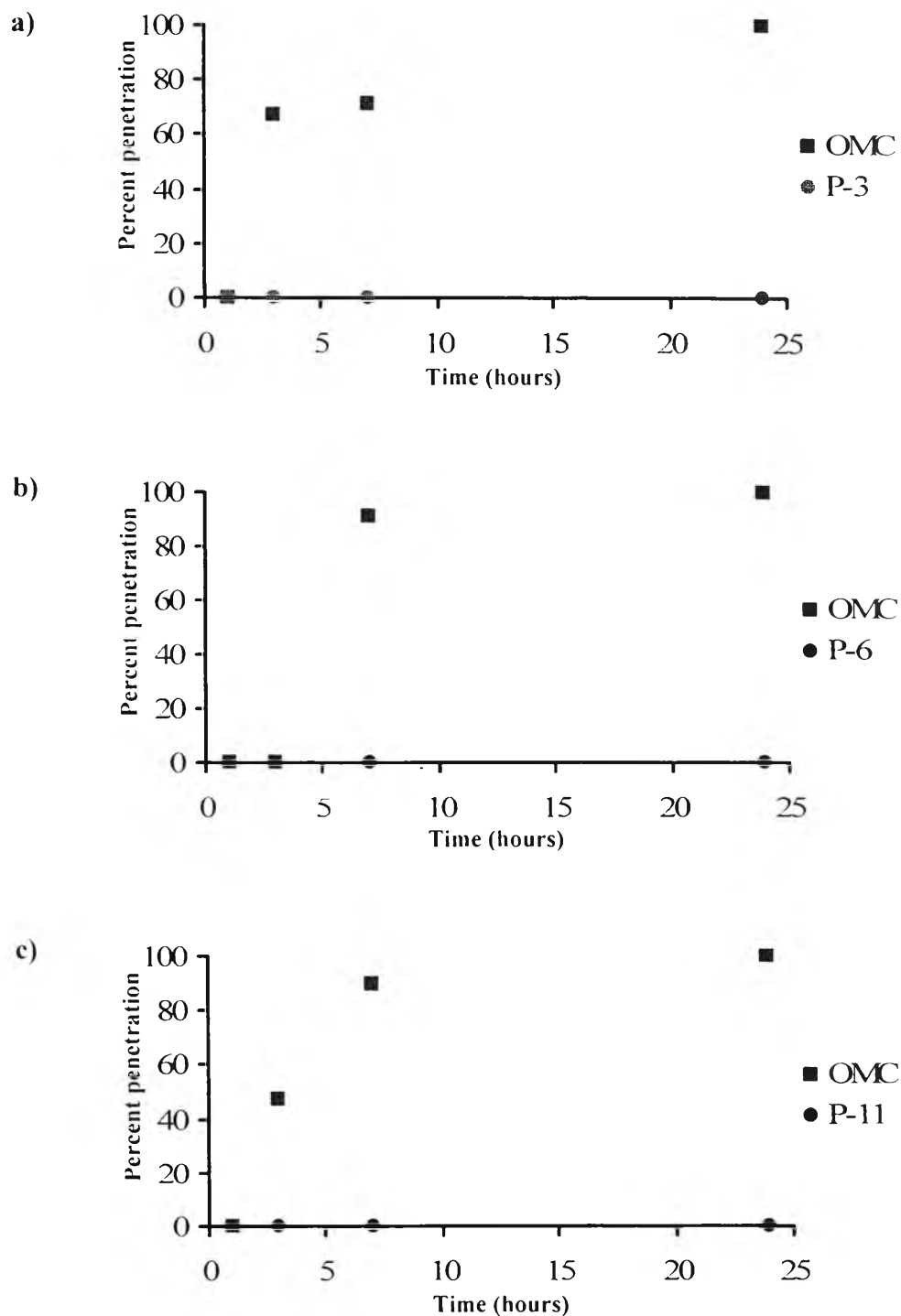


**Figure 3.10** Penetration of OMC compared with synthesized UV-filter polymers into receptor fluid: a) P-3, b) P-6, c) P-11, d) P-3/11 and e) PPGC

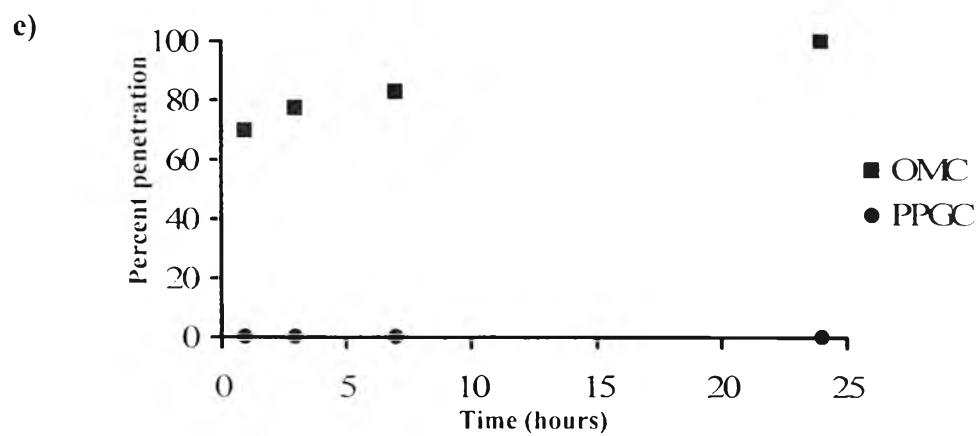
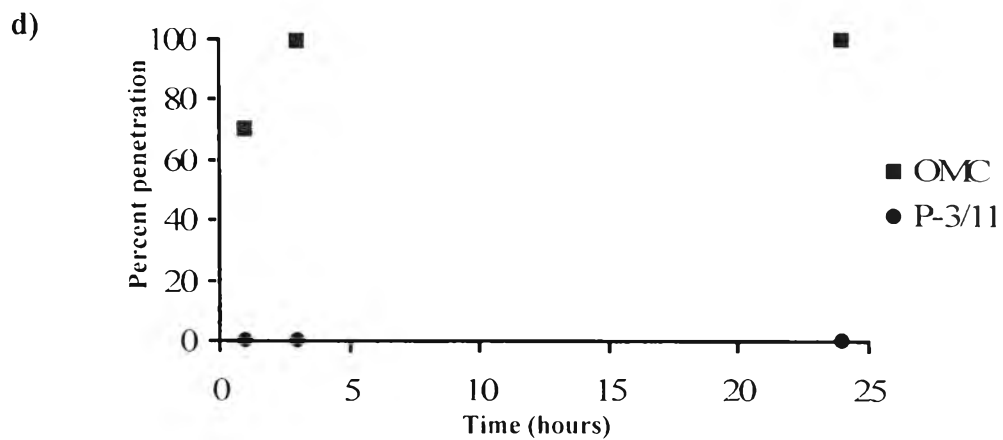


**Figure 3.10** Penetration of OMC compared with synthesized UV-filter polymers into receptor fluid: a) P-3, b) P-6, c) P-11, d) P-3/11 and e) PPGC